
ELSEVIER
ISSN 0022-4804
Volume 178
Number 2
December 2012
JSR
Journal of
Surgical Research
Official Publication of the
Association for Academic Surgery
Full-Text and Submit Manuscripts:
www.JournalofSurgicalResearch.com

JOURNAL OF SURGICAL RESEARCH 178 (2012) 533–538

Available online at www.sciencedirect.com

SciVerse ScienceDirect

journal homepage: www.JournalofSurgicalResearch.com

Rapid screening of cancer margins in tissue with multimodal confocal microscopy

Daniel S. Gareau, PhD,[a,b,*] *Hana Jeon, MD,*[a] *Kishwer S. Nehal, MD,*[a] and *Milind Rajadhyaksha, PhD*[a]

[a] *Dermatology Service, Memorial Sloan-Kettering Cancer Center, 160 East 53rd Street, New York 10022, New York*
[b] *Department of Investigative Dermatology, The Rockefeller University, New York, New York*

ARTICLE INFO

Article history:
Received 23 February 2012
Received in revised form
16 May 2012
Accepted 17 May 2012
Available online 7 June 2012

Keywords:
Confocal microscopy
Mohs surgery
Margin screening
Pathology
Basal cell carcinoma

ABSTRACT

Background: Complete and accurate excision of cancer is guided by the examination of histopathology. However, preparation of histopathology is labor intensive and slow, leading to insufficient sampling of tissue and incomplete and/or inaccurate excision of margins. We demonstrate the potential utility of multimodal confocal mosaicing microscopy for rapid screening of cancer margins, directly in fresh surgical excisions, without the need for conventional embedding, sectioning, or processing.

Materials and methods: A multimodal confocal mosaicing microscope was developed to image basal cell carcinoma margins in surgical skin excisions, with the resolution that shows nuclear detail. Multimodal contrast is with fluorescence for imaging nuclei and reflectance for cellular cytoplasm and dermal collagen. Thirty-five excisions of basal cell carcinomas from Mohs surgery were imaged, and the mosaics analyzed by comparison with the corresponding frozen pathology.

Results: Confocal mosaics are produced in about 9 min, displaying tissue in fields of view of 12 mm with ×2 magnification. A digital staining algorithm transforms black and white contrast to purple and pink, which simulates the appearance of standard histopathology. Mosaicing enables rapid digital screening, which mimics the examination of histopathology.

Conclusions: Multimodal confocal mosaicing microscopy offers a technology platform to potentially enable real-time pathology at the bedside. The imaging may serve as an adjunct to conventional histopathology to expedite screening of margins and guide surgery toward more complete and accurate excision of cancer.

1. Introduction

Precise and complete excision of cancer is guided by the examination of margins with histopathology during surgery. The preparation of histopathology, however, is labor intensive and time consuming. For example, Mohs surgery is a tissue-sparing procedure for nonmelanoma skin cancers [1–3] that is guided by the examination of frozen sections of excision margins. Multiple serial excisions are often necessary to achieve cancer-free margins, with frozen tissue preparation requiring 20–45 min for each excision [4]. In the general surgery setting, however, the preparation of frozen sections is often not possible, and the final margin status is determined with fixed tissue sections, which typically requires several days to prepare.

* *Corresponding author*. 1230 York Avenue, Mailbox 178, New York, NY 10065, USA. Tel.: +1 212 327 7983; fax: +1 212 327 8232.
E-mail address: dgareau@rockefeller.edu (D.S. Gareau).
0022-4804/$ – see front matter © 2012 Elsevier Inc. All rights reserved.
doi:10.1016/j.jss.2012.05.059

Consequently, sampling of tissue during surgery is often insufficient, and cancer margins remain incompletely excised in patients, who must subsequently return for re-excision and/or chemotherapy and/or radiotherapy. Recent studies report that 20%–70% of patients undergoing breast cancer lumpectomy may be recalled for re-excision [5]. After head and neck surgery, 15%–50% of patients may present with positive margins and undergo subsequent radiotherapy and/or chemotherapy [6]. The rate of re-excision for positive margins for nonmelanoma skin cancers can be 32%–39% after surgical excision [7]. For cutaneous squamous cell carcinomas, the re-excision rate can be 17% after the initial surgery and 28% after the second surgery [8].

The preparation of histopathology requires a laboratory with specialized personnel and expertise and associated expense. For example, for 1 million Mohs surgeries performed every year in the United States alone, the total treatment cost exceeds $1 billion [9,7]. About 10%–20% of the total cost is related to preparation of frozen histopathology, which amounts to about $100–200 million/y. In other surgical settings, the need for subsequent re-excision and/or therapy increases the cost with additional procedures and pathology. In today's environment, the medical profession is facing increasing demands to provide increasingly efficient care at increasingly lower costs. Toward addressing these issues, emerging innovations in noninvasive optical imaging technologies may prove useful. One such emerging technology is confocal mosaicing microscopy that images nuclear and cellular details, similar to that seen in histopathology, but directly in fresh tissue, without the need for any processing. Confocal mosaicing microscopy was originally developed for detecting basal cell carcinomas (BCCs) in Mohs surgical skin excisions [4,10–12] and more recently for the detection of ductal carcinomas *in situ* and invasive lobular carcinomas in breast biopsies [13,14].

A confocal microscope noninvasively images a thin plane directly in fresh tissue without the need for traditional grossing, embedding, physical sectioning, and staining [15]. Noninvasive imaging of thin planes within the whole tissue is called "optical sectioning" and may be performed directly on patients *in vivo* or in freshly excised tissue *ex vivo*. Nuclear and cellular details are observed in thin optical sections of 1–3 μm, with 0.5–1.0 μm resolution. The optical sectioning and resolution are comparable to the typical 5-μm thin tissue sections that are prepared for histopathology. However, in microscopy, the physics of light fundamentally restrict the ability to perform optical sectioning at high resolution to relatively small fields of view of up to 1 mm. To increase the field of view, a two-dimensional sequence of images may be acquired and stitched, in software, into a mosaic [4,10–12]. Mosaics display large areas of tissue at varying magnifications of ×2 to ×30, analogous to that provided by microscope objectives when viewing pathology.

Clinical imaging of skin excisions is an excellent model for testing confocal microscopy and producing a technology platform for translation to other tissues. Feasibility of screening cancer margins, with fluorescence confocal mosaicing microscopy, has been demonstrated for BCCs in Mohs surgical skin excisions [4,10–12]. Acridine orange was used to stain nuclei in fluorescence contrast, and BCCs were detected with a sensitivity of 96.6% and specificity of 89.2% [16,17]. Although these results are promising, barriers toward routine clinical use may be anticipated. Confocal mosaics thus far [16,17] have been based on a single mode of contrast (fluorescence) and have appeared in grayscale (black and white), whereas histopathology stained with hematoxylin and eosin (H&E) is based on two agents, with hematoxylin staining nuclei purple and eosin staining cytoplasm pink. The grayscale (black and white) appearance of confocal mosaics may pose limitations for acceptance by surgeons and pathologists, who, of course, are trained and accustomed to the purple and pink appearance of histopathology.

Toward addressing this barrier, we report an advance in confocal mosaicing microscopy: a multimodal imaging system with digital staining to transform grayscale black and white contrast to purple and pink, to mimic the appearance of H&E-stained histopathology. Multimodal refers to two modes of contrast: fluorescence contrast to highlight nuclear morphology and reflectance contrast to highlight cellular cytoplasm and dermal morphology. Feasibility is demonstrated for the detection of BCC margins in Mohs surgical skin excisions.

2. Materials and methods

In the Mohs surgery setting, fresh frozen tissue that remains after the preparation of histopathology is routinely discarded. Discarded tissue specimens were collected from 35 cases, under an institutional review board–approved protocol. The frozen tissue specimens were thawed and rinsed with isotonic saline. Acridine orange solution of concentration 1 mM, in phosphate-buffered saline at pH 6.0, was used to stain nuclei. As described in our earlier articles [11], the tissue specimens were immersed in acridine orange for 20 s and then rinsed in saline to wash off any unbound excess. This staining procedure does not have any adverse effect on subsequent frozen Mohs histopathology [11]. The specimens are mounted in a tissue fixture in the confocal microscope, in a manner that mimics the conventional process of mounting Mohs surgical excisions in a cryostat when preparing frozen sections. The tissue fixture was specially designed and engineered for mounting of Mohs surgical excisions [10].

A research breadboard version of a commercially available reflectance confocal microscope (Vivascope 2000; Lucid Inc., NY) was modified to incorporate imaging in fluorescence and mosaicing capability, and details are available elsewhere [11]. Briefly, the microscope is equipped with a 40 mW, 488 nm Argon-ion laser (Omnichrome; CVI Melles Griot Inc., Carlsbad, CA) for illumination and two detection channels for fluorescence and reflectance with avalanche photodiode detectors (Perkin-Elmer, Quebec, Canada). Images were acquired at the rate of 20 frames/s. Imaging was performed using a ×30, 0.9 numerical aperture objective lens (Stableview; Lucid Inc) and a water-based gel (Suave Naturals, Unilever, Englewood Cliffs, NJ) as an immersion medium. With this lens, the estimated optical sectioning is ∼1 μm, and the lateral resolution is ∼0.3 μm. With the tissue fixture on a translation stage and using a step-and-capture algorithm, up to 36 × 36 images were acquired, processed, and stitched into a mosaic with an algorithm developed in Matlab (Mathworks Inc, Natick, MA) [11]. Mosaics display a large field of view in which nuclear detail is visualized. This field of view corresponds to a magnification of ×2, as on a standard microscope. Currently, confocal mosaics that display up to 12 × 12 mm of tissue can be produced in about 9 min. Coregistered mosaics were acquired using both the reflectance and fluorescence channels of the multimodal confocal microscope, as described previously [11]. Digital staining was implemented on the reflectance and fluorescence mosaics to simulate H&E-like appearance.

Digital staining transforms the grayscale fluorescence and reflectance pixel intensities into corresponding red, green, and blue levels [18], according to the equation: $I_{x,y,k} = 1 - F_{x,y}(1 - H_k) - R_{x,y}(1 - E_k)$. The digitally stained image ($I_{x,y,k}$) is a linear combination of the fluorescence ($F_{x,y}$) and reflectance ($R_{x,y}$) mosaics. In this equation, $F_{x,y}$ are the pixel grayscale values for nuclei in the fluorescence mosaic and $R_{x,y}$ are for cellular cytoplasm and collagen in the reflectance mosaic. F and R were single values for each pixel, normalized to make the brightest pixel unity. The subscripts x and y denote the pixel location in the mosaic, and the subscript k denotes the bit depth for red ($k = 1$), green ($k = 2$), and blue ($k = 3$) channels of the digitally stained image. The relative red, green, and blue components to mimic H&E-like appearance were determined from a digital image of a conventional H&E-stained Mohs frozen section by sampling one typical pixel in the hematoxylin-stained area and one in the eosin-stained area. The red, green, and blue (R, G, and B) components obtained to approximate H&E colors were $H = (0.30, 0.20, \text{and } 1)$ and $E = (1, 0.55, \text{and } 0.88)$.

Application of the equation to each pixel of the grayscale images yields the digitally stained image, in which nuclei appear purple and collagen and cytoplasm appear pink. The reflectance and fluorescence brightness in confocal images are inverted to the absorbance-based contrast that is seen in histopathology, which is familiar to surgeons and pathologists. In the absence of a fluorescent or reflectance signal, $R = F = 0$ such that the digitally stained image $I_{x,y,k}$ is unity, which mimics the white background in conventional H&E histopathology. When R and F are not zero, their magnitude determines the suppression of brightness (i.e., absorbance) in $I_{x,y,k}$. If the density of contrast agent (i.e., fluorescent acridine orange molecules that are bound to the nuclei or reflective structures such as cytoplasmic organelles or collagen) is high, the F or R values in the fluorescent and reflectance confocal mosaics are high (i.e., bright on a dark background), and the corresponding digitally stained image appears dark or colored on a bright background.

The digitally stained mosaics were displayed, for examination by the Mohs surgeon, on a 30-inch flat screen monitor (Dell 222-7175 with a GeForce 8800 GTS video card, Dell Inc, Round Rock, TX) consisting of 2500 × 1600 pixels. The pixilation of this monitor mimics that in a ×2 magnified view of histopathology in a standard microscope. Zoom and pan capabilities, similar to those in today's digital cameras, allow areas of interest to be viewed with variable magnification of ×2 to ×30, while maintaining resolution for visualizing nuclear detail. The digital display and observation of mosaics thus mimic the Mohs surgeon's routine for examination of histopathology.

Of the 35 cases, 14 were discarded because of poor quality (inconsistent registration, stitching, and appearance) of the reflectance mosaics. The remaining 21 contained BCC margins with varying tumor burden, from grossly positive (i.e., >90%) to largely tumor-free (i.e., <10%). These mosaics were presented to the Mohs surgeon for the evaluation of image quality (consistent contrast and seamless mosaic stitching) and screening while remaining "blinded" to the histopathology. The evaluation for the presence or absence of BCC margins was subsequently compared with the corresponding frozen pathology.

3. Results

Fig. 1 shows an example of a digitally stained confocal mosaic (Fig. 1a) and the corresponding H&E-stained Mohs frozen histopathology (Fig. 1b) at ×2 magnification. In the mosaic, nuclei appear purple, whereas cellular cytoplasm and collagen appear pink comparable to the appearance in standard H&E-stained Mohs histopathology. Normal skin structures such as the epidermis and dermis containing hair follicles, sebaceous glands, and collagen are easily recognized. Aggregates of BCC tumors displaying nodular, micronodular, and infiltrative subtypes with associated inflammatory infiltrate are readily distinguished from the normal structures. Nuclear and morphologic details may not be easily appreciated in the small figure in this article but is readily seen on our large monitor. The details will be more evident in the smaller portions of the mosaic (i.e., insets in Fig. 1) that are shown in Figs 2 and 3.

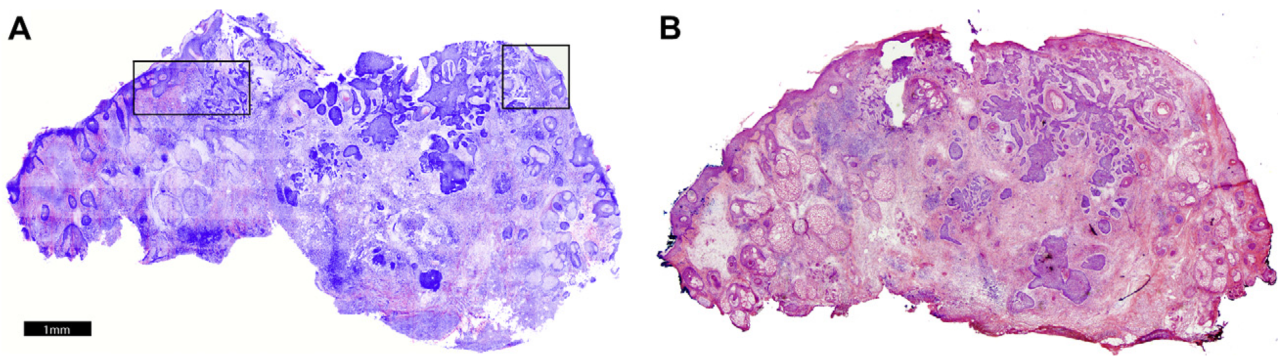

Fig. 1 – (A) Digitally stained confocal mosaic with residual BCC compares well with (B) Mohs H&E-stained frozen section histopathology (magnification ×2). To make the details more evident, two inset areas are shown at higher magnifications: the upper left at ×10 (Fig. 2) and the upper right at ×20 (Fig. 3).

Fig. 2 highlights the production process of a digitally stained confocal mosaic. The exogenous fluorescence mode (Fig. 2a) with acridine orange displays bright nuclei, which are digitally stained purple. The endogenous reflectance mode (Fig. 2b) shows predominantly cellular cytoplasm and collagen in the dermis, which is digitally stained pink. Fig. 2c shows the resulting mosaic, which compares well, overall, with the corresponding Mohs histopathology (Fig. 2d) for the presence and appearance of BCC tumor, normal epidermis, and associated features.

Fig. 2 also demonstrates digital "zooming" into the mosaic, which allows observation of tissue in submosaics at a higher magnification of ×10, while maintaining full resolution and pixelation. The malignant nuclear morphology of BCC (Fig. 2c) such as nuclear pleomorphism, increased nuclear density, and peripheral palisading is visualized with the definition similar to that (Fig. 2d) seen in the Mohs H&E-stained histopathology. Fig. 3 shows these details at higher magnification of ×20, along with the corresponding histopathology.

The appearance of the hematoxylin-stained purple-appearing nuclei is reasonably consistent, but the eosin-stained pink-appearing dermis is more variable. This variability appears to be because of the presence of small amounts of acridine orange that may not be completely washed out, resulting in an exogenous fluorescence signal that contaminates the endogenous reflectance image. Thus, there is a purplish component in the dermis that obscures the pink in some mosaics (Fig. 1). Elastin fibrils are occasionally stained by acridine orange, leading to a purple fibrous component in the dermis, particularly with solar elastosis in aged and sun-damaged skin. In such cases, the delineation between elastosis and healthy collagen was uncertain. Other artifacts include saturated fluorescence contrast resulting from excess pooling of the acridine orange and/or high laser power.

The consistency of the contrast in the reflectance mode suffered only when the imaging plane was too superficial, picking up artifact reflectance from the glass window onto which the Mohs excision was placed. The consistency of contrast in the fluorescence mode suffered with uneven staining such that, in some areas, the nuclear morphology was too bright (saturated), and, in other areas, too dim (faded). In the review by the Mohs surgeon (coauthor K.S.N.), who compared the confocal mosaics against the expectations of histology, 9 of the 21 were deemed to be of "poor" quality, 8 were of "medium" quality, and 4 were of "good" quality.

The screening results for the 21 mosaics (all 21 mosaics contained BCC tumor in the surgical margins) were as follows: 17 positive and four negative. The four mosaics, in which BCCs were present but not identified by the Mohs surgeon, were all cases of very low tumor burden. The fractions of the images that contained tumor within the mosaics were 3/150, 1/350, 4/450, and 2/150, indicating tumor burden of 0.3%–2%. Two of these four cases were superficial, in which the BCC was budding off the epidermis, and two were micronodular with just one small tumor focus in the dermis. In three of the four cases that were misread as negative, the quality of the staining was poor: The acridine orange fluorescence (depth of the purple color) showing nuclear detail was weak compared with the strong reflectance (pink) color that showed cellular and dermal collagen details.

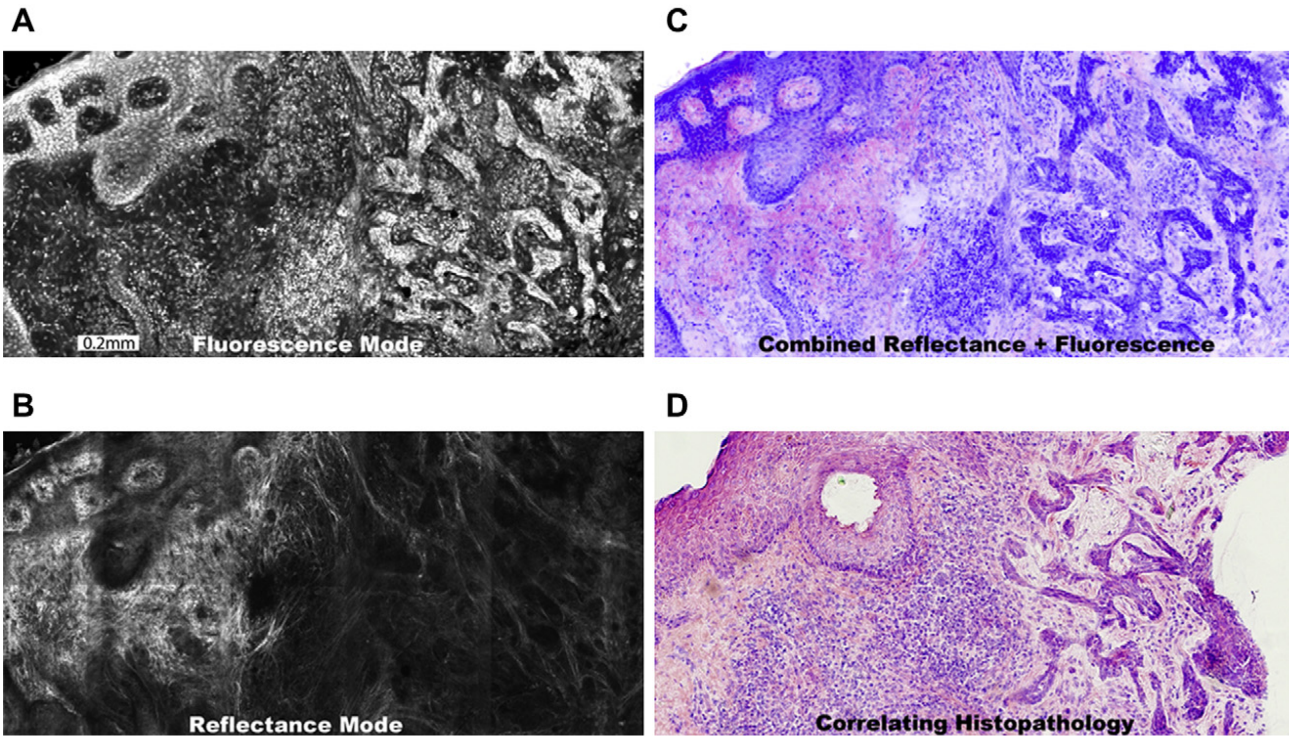

Fig. 2 – A digitally stained confocal mosaic is composed of an (A) exogenous fluorescent mosaic showing nuclei stained with acridine orange that is combined with an (B) endogenous reflectance mosaic showing cellular cytoplasm and collagen. (C) The fluorescence mosaic is digitally stained purple, and the reflectance pink and the two are overlaid to produce the digitally stained mosaic. (D) The mosaic appears comparable to the H&E-stained histopathology (magnification ×10) for the presence and appearance of BCC tumor, normal epidermis, and associated features. The features are further described in Fig. 3.

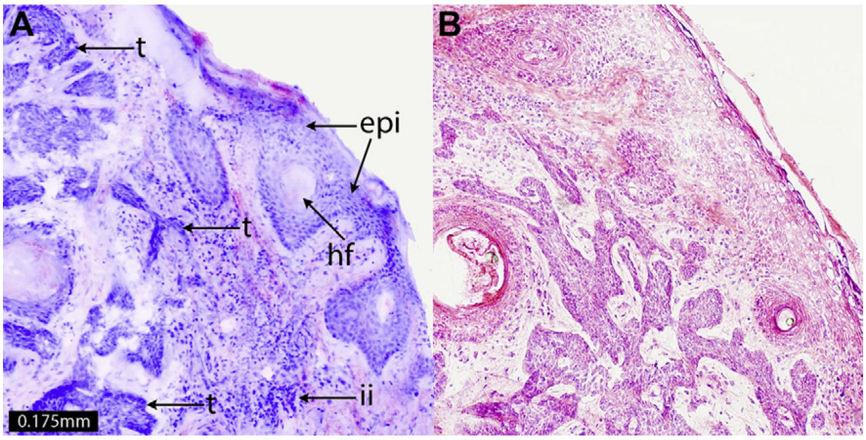

Fig. 3 – (A) A digitally stained confocal submosaic shows details of features at ×20 magnification that include the epidermis along the edges of the tissue (epi), hair follicle (hf), inflammatory infiltration (ii), and micronodular BCC tumor (t). (B) These features appear similar to those seen in the corresponding H&E-stained histopathology (magnification ×20). Such features are routinely examined in Mohs pathology.

Thus, the conclusion from this preliminary clinical review is that the technology—methods for preparation of mosaics and digital staining—must be further improved to subsequently allow a rigorous study of sensitivity and specificity.

4. Discussion

Previously, in purely reflectance contrast [10,12] with the use of acetic acid (acetowhitening) to brighten nuclear morphology, large nodular BCC tumors could be detected, but because the tumors were not many fold brighter than the background dermis, small tumors such as micronodular, infiltrating, and sclerosing BCCs remained hidden in the mosaic's large field of view. Subsequently, in purely fluorescence contrast with the use of acridine orange, all subtypes of BCC tumors were detected [11]. Sensitivity and specificity were shown to be 96.6% and 89.2%, respectively [16,17]. Despite the high sensitivity and specificity, black and white (grayscale) images pose a possible barrier to clinical acceptance in that they lack the familiar appearance that surgeons and pathologists are accustomed to; hence, retraining is necessary. To address this limitation, we developed a digital staining approach [18].

This study represents the first step toward a preclinical analysis of multimodal mosaics that appear in purple and pink contrast, similar to that of conventional H&E-stained histopathology, instead of the usual black and white (grayscale) that is commonly seen in confocal microscopy. In our results, unevenness of staining represents a major limitation. The staining protocol needs to be improved to enable consistently strong nuclear contrast. In addition, work is also necessary to improve both the mosaicing approach and the multimodal digital staining approach.

Our ongoing research and engineering are therefore focused on five areas: (i) improvements in image alignment, registration, and stitching to produce consistently high quality and clinically acceptable mosaics; (ii) optimization of the fluorescence staining technique with acridine orange to reduce the purple-staining artifacts in the dermis; (iii) spectral classification analysis of hematoxylin- and eosin-stained tissues to lead to a better understanding of the staining process in histopathology and subsequent improvement in our digital staining algorithm[19]; (iv) refinements in the tissue fixture to enable use for a diverse variety of excision sizes and shapes in diverse surgical and clinical settings; and (v) development of a "strip mosaicing" approach that will allow display of larger areas of tissue in shorter times, by stitching together long strips of images, similar to the operation in a document scanner [20]. Preliminary results suggest that up to 25 × 25 mm (1 × 1 inch) of tissue may be mosaiced in 2–3 min.

The limitations of "static" mosaicing in this study may be alleviated with "live" confocal microscopy, where the surgeon would be able to interrogate the tissue in real-time during surgery. While observing a "live" mosaic, regions of uncertainty or artifact could be further investigated by imaging deeper into the tissue, in a manner that mimics the examination of additional sections in histopathology. For example, the uncertain differentiation between hair follicles *versus* micronodular BCCs in Mohs surgery is traditionally addressed by viewing successive frozen sections in depth. Correspondingly, in a "live" mosaic, the optical section may be focused deeper for real-time observation to depths of 50–100 μm, which would be the equivalent of examining 10–20 histopathology sections.

The present research in skin tissue from Mohs surgery demonstrates proof of concept and the possible utility of high-speed large-area mosaicing in many other surgical and clinical settings to examine freshly excised tissue. The technology may enable rapid pathology at the bedside to potentially expedite and guide surgery or biopsy. Additionally, the images and mosaics are in a digital format that is ideal for telepathology, which continues to be developed and increasingly implemented worldwide [21,22]. Confocal mosaicing microscopy may evolve into a powerful adjunct or, perhaps, an entirely new alternative to histopathology.

Beyond mosaicing in excised tissue, confocal imaging may be performed directly on the patient, preoperatively and intraoperatively. Our preliminary study indicates the feasibility of detecting residual nonmelanoma skin cancers in patient wounds after shave biopsies [23]. We recently initiated a follow-up study to test the feasibility of confocal mapping of nonmelanoma skin cancer margins in patients during Mohs surgery. Ultimately, the best approach may involve clever combinations of "live" mosaicing at the bedside and intraoperative mapping on the patient, configured as needed for any given setting. With further refinements of this technology to facilitate ease of use, surgeons and clinicians may be empowered to perform more complete screening of margins in a fast, efficient, and cost-effective manner.

Acknowledgment

The authors thank Mohs histology technicians Marie Tudisco and Barbara Strippoli for their help with the frozen histology and intellectual involvement with this research. The authors are grateful to Jay Eastman and William Fox of Lucid Inc for their technical support. This work was funded mainly by National Institutes of Health (R01EB002715). Additional funding was provided by a grant from the Byrne Fund (Department of Medicine at MSKCC).

REFERENCES

[1] Minton TJ. Contemporary Mohs surgery applications. Curr Opin Otolaryngol Head Neck Surg 2008;16:376.
[2] Cumberland L, Dana A, Liegeois N. Mohs micrographic surgery for the management of nonmelanoma skin cancers. Facial Plast Surg Clin North Am 2009;17:325.
[3] Perkins W. Who should have Mohs micrographic surgery? Curr Opin Otolaryngol Head Neck Surg 2010;18:283.
[4] Rajadhyaksha M, Menaker G, Flotte TJ, et al. Rapid confocal examination of nonmelanoma cancers in skin excisions to potentially guide Mohs micrographic surgery. J Invest Dermatol 2001;117:1137.
[5] Jacobs L. Positive margins: the challenge continues for breast surgeons. Ann Surg Oncol 2008;15:1271.
[6] Haque R, Contreras R, McNicoll MP, Eckberg EC, Petitti DB. Surgical margins and survival after head and neck cancer surgery. BMC Ear Nose Throat Disord 2006;6:2. doi:10.1186/1472-6815-6-2. Available: http://www.biomedcentral.com/1472-6815/6/2. Accessed July 12, 2012.
[7] Tierney EP, Hanke CW. Cost effectiveness of Mohs micrographic surgery: review of the literature. J Drugs Dermatol 2009;8:914.
[8] Bovill ES, Cullen KW, Barrett W, Banwell PE. Clinical and histological findings in re-excision of incompletely excised cutaneous squamous cell carcinoma. J Plast Reconstr Aesthet Surg 2009;62:457.
[9] Bialy TL, Whalen J, Veledar E, et al. Mohs micrographic surgery versus traditional surgical excision—a cost comparison analysis. Arch Dermatol 2004;140:736.
[10] Patel YG, Nehal KS, Aranda I, Li Y, Halpern AC, Rajadhyaksha M. Confocal reflectance mosaicing of basal cell carcinomas in Mohs surgical skin excisions. J Biomed Opt 2007;12:034027.
[11] Gareau DS, Li Y, Huang B, Eastman Z, Nehal KS, Rajadhyaksha M. Confocal mosaicing microscopy in Mohs skin excisions: feasibility of rapid surgical pathology. J Biomed Opt 2008;13:054001.
[12] Gareau DS, Patel YG, Li Y, et al. Confocal mosaicing microscopy in skin excisions: a demonstration of rapid surgical pathology. J Microsc 2009;233:149.
[13] Schiffhauer LM, Boger JN, Bonfiglio TA, Zavislan JM, Zuley M, Fox CA. Confocal microscopy of unfixed breast needle core biopsies: a comparison to fixed and stained sections. BMC Cancer 2009;9:265.
[14] Maddalena TT, Cabrera MC, Parrish AR, et al. Real-time imaging and characterization of human breast tissue by reflectance confocal microscopy. J Biomed Opt 2007;12:051901.
[15] Gonzalez S, Gill M, Halpern AC, editors. Reflectance confocal microscopy of cutaneous tumors. London: Informa U.K. Ltd; 2008.
[16] Gareau DS, Karen JK, Dusza SW, Tudisco M, Rajadhyaksha M, Nehal KS. Sensitivity and specificity for detecting basal cell carcinomas in Mohs excisions with confocal fluorescence mosaicing microscopy. J Biomed Opt 2009;14:034012.
[17] Karen JK, Gareau DS, Dusza SW, Tudisco M, Rajadhyaksha M, Nehal KS. Detection of basal cell carcinomas in Mohs excisions with fluorescence confocal mosaicing microscopy. Br J Dermatol 2009;160:1242.
[18] Gareau DS. The feasibility of digitally stained multimodal confocal mosaics to simulate histopathology. J Biomed Opt 2009;14:034050.
[19] Bini J, Spain J, Nehal K, Hazelwood V, DiMarzio C, Rajadhyaksha M. Confocal mosaicing microscopy of human skin *ex vivo*: spectral analysis for digital staining to simulate histology-like appearance. J Biomed Opt 2011;16:076008. doi: 10.1117/1.3596742. Accessed July 12, 2012.
[20] Abeytunge S, Li Y, Larson B, Toledo-Crow R, Rajadhyaksha M. Rapid confocal imaging of large areas of excised tissue with strip mosaicing. J Biomed Opt 2012;16:050504.
[21] Weinstein RS, Graham AR, Richter LC, et al. Overview of telepathology, virtual microscopy, and whole slide imaging: prospects for the future. Hum Pathol 2009;4:1057.
[22] Jara-Lazaro AR, Thamboo TP, Teh M. Digital pathology: exploring its applications in diagnostic surgical pathology practice. Pathology 2010;42:512.
[23] Scope A, Mahmood U, Gareau DS, et al. *In vivo* reflectance confocal microscopy of shave biopsy wounds: feasibility of intraoperative mapping of cancer margins. Br J Dermatol 2010;163:1218.